Low-cost high-sensitive Suns-V_{oc} measurement instrument to characterize c-Si solar cells

Pablo R. Ortega, Juan M. Piñol*, Isidro Martín, Albert Orpella, Gerard Masmitjà, Gema López, Eloi Ros, Cristobal Voz, Joaquim Puigdollers, Ramón Alcubilla

Departament d'Enginyeria Electrònica, Universitat Politècnica de Catalunya (UPC)
Micro and Nanotechnologies Group, MNT
Barcelona, Spain

* Now with Idneo Technologies SAU,
Mollet del Vallès, Barcelona, Spain

Abstract

Measuring open-circuit voltage (V_{oc}) vs. light intensity (Suns) in solar cells permits the access of cell performance without the series resistance effect. This work shows the implementation of a Suns-V_{oc} measurement system which consists of an off-the-shelf photograph flash-lamp, a digital oscilloscope and a specifically designed photodetector board with three silicon photodiodes that covers a light intensity measurement range from 10^{-5} to 10^{2} suns. The whole system is controlled via USB ports from a personal computer allowing the measurement of cell characteristics (pseudo-dark and pseudo-light current density-voltage curves, as well as the pseudo fill factor and pseudo efficiency) automatically in a very short time.

Index Terms— Suns-V_{oc} method, solar cells, crystalline silicon, pseudo fill factor, series resistance, flash lamp

I. INTRODUCTION

To make solar cells competitive against conventional energy sources a cost-effective approach must be followed along all the value chain, including their characterization [1-4]. Quasi-steady-state Suns-open circuit voltage measurement method (QSS-V_{oc}) is a popular technique to characterize the electrical performance of solar cells without considering the contribution of series ohmic losses [5, 6]. While Suns-V_{oc} characterization is more commonly used in crystalline silicon (c-Si) solar cells [7], this technique is now widely used in the photovoltaic (PV) community applied to different technologies like III-V alloy compounds [8], organic [9], kesterite [10] and thin-film polycrystalline silicon on glass [11] solar cells.

In this characterization method, the solar cell is illuminated with a time-varying light intensity, typically from a flash-lamp to prevent heating up the sample. The open circuit voltage of the solar cell (V_{oc}) and the irradiance level time dependence are measured together using two channels of a digital oscilloscope, as it is shown in Fig.1. One oscilloscope channel is directly connected to the solar cell under open circuit conditions measuring the V_{oc} parameter, while the other channel simultaneously measures the corresponding irradiance level from the flash lamp light using a photodetector circuit, channel I and II respectively in Fig. 1. By processing both signals, the static pseudo-dark and pseudo-light current-voltage characteristics without ohmic losses, pJ_{dark}-V_{oc} and pJ_{light}-V_{oc} curves respectively, can be obtained. Additionally, important electrical/physical parameters of the solar cell as the pseudo Fill Factor (pFF), or the pseudo efficiency ($p\eta$) can be easily extracted. Moreover, this technique allows to get effective lifetime information once the device is finished. This last parameter is crucial for a correct development of the devices and it can be measured during fabrication process through photoconductance techniques [12, 13], which becomes impracticable with metal contacts. Impedance spectroscopy has been proposed as an alternative, but with complex models and time consuming techniques [14].

Commercial Suns-V_{oc} systems are available [15], but with important limitations. A part from the system cost, at least ten times higher than the approach reported in this work, they are designed for double side contacted solar cells which makes difficult to measure solar cells with other contact structure, e.g. interdigitated back contact (IBC) devices

where all the contacts are located at the rear face of the device. Additionally, light intensity can be changed from 0.006 to 6 suns [15] introducing neutral optical filters which is a very time consuming method. Moreover, important information is located at lower irradiance levels leading to more reliable data of the recombination processes, i.e. effective lifetime values, occurring at low injection levels.

In this work, we propose a low-cost, user-friendly and flexible Suns-V_{oc} instrument with a wide measurement range from 10^{-5} to 10^{2} suns in the irradiance level using six measurement scales. The measurement process is performed automatically with six flash shots in less than 1 min. After the measurement, all curves and parameters involved in Suns-V_{oc} measurements are calculated and shown to the final user, being a very useful tool to optimize the design and the fabrication process involved in different solar cell structures.

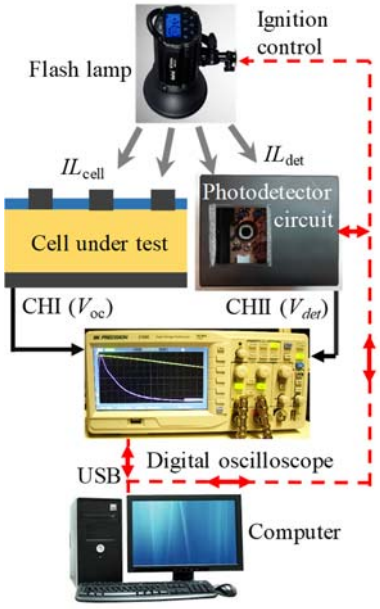

Fig. 1. (color online) Main components in the QSS-V_{oc} measurement system. Dashed red lines correspond with control/communication lines between the involved elements.

II. SUNS-VOC TECHNIQUE FUNDAMENTALS

Suns-V_{oc} measurements allow to obtain both dark and light current-voltage static characteristics of a solar cell without considering series ohmic losses in the so called

pseudo-dark and pseudo-light current density vs. open circuit voltage curves, pJ_{dark}-V_{oc} and pJ_{light}-V_{oc} curves respectively. In order to understand the working principles of this method, we can use a dynamic electrical model of a solar cell including series resistance R_s. This model is shown in Fig. 2a where. J_{ph} is the generated photocurrent which is assumed to be proportional to the measured irradiance level on the cell (IL_{cell}). Notice that IL_{cell} is obtained by means of the photodetector circuit as it is explained in section III. The J_{dark} term (current flowing through the gray-filled block in Fig. 2) is the diode dark static current density without series resistance losses, while V' is the voltage dropped through the junction. The non-linear voltage-dependent capacitance (C_D) is introduced in the electrical solar cell model in order to take into account the dynamics of the excess carrier densities in the quasi-neutral absorber regions of the device. This capacity value per unit area can be deduced from the Kerr's work [5] applied to silicon solar cells as

$$C_D(V') = \frac{qw n_i^2 e^{\frac{V'}{V_T}}}{V_T \sqrt{N_{Dop}^2 + 4n_i^2 e^{\frac{V'}{V_T}}}} \quad (1)$$

where q, n_i, w, N_{dop}, and V_T are the elementary charge, the intrinsic concentration ($9.56 \cdot 10^9$ cm^{-3} at 25ºC), the device thickness, the doping on the absorber region and the thermal voltage (25.69 mV at 25ºC), respectively.

Equation (1) assumes a uniform carrier excess profile inside the absorber region, i.e. both bulk and surface recombination are low. It is important to comment that the impact of the C_D element in the QSS-V_{oc} measurements is high for slow response solar cells, i.e. very well passivated devices with long effective lifetimes (τ_{eff}) in comparison with the light decay time of the flash lamp (τ_{Flash}) [5]. In that case, the aforementioned assumption of a uniform carrier excess profile holds leading to an accurate value for C_D. On the contrary, for τ_{eff} much lower than τ_{Flash}, Suns-V_{oc} measurements scarcely depend on the cell dynamics since excess carrier densities rapidly vanish and capacitive behavior can be neglected. Therefore, although equation (1) could be inaccurate for C_D calculation, this parameter does not have any impact. As a consequence, equation (1) can be applied to the calculation of C_D in any case.

From Fig. 2.a, we can see that it is possible to define a net current density (J_{net}) by grouping the photocurrent (J_{ph}) with the current density flowing through C_D capacitor (J_c) as follows:

$$J_{net} = J_{ph} - J_c = IL_{cell} \times J_{ph,cell}(1Sun) - C_D \frac{dV'}{dt} \quad (2)$$

being $J_{ph,cell}$ (1Sun) the cell photocurrent measured at one sun (AM1.5G 1 kW/m^2 solar spectrum) and IL_{cell} in Suns units.

It is clear, from Fig. 2c, that in open-circuit conditions the voltage *V'* is the same as the open circuit voltage of the cell. Simultaneously, J_{net} equals the current through the device that in that case is known as pseudo-dark current density (pJ_{dark}). In other words, we are biasing the device not by externally introducing current, but by illuminating it, avoiding in this way the effect of R_s. Following this idea, from eq. (2) we can define an interesting magnitude called effective net irradiance level (IL_{net}). Assuming that J_{net} is proportional to IL_{net}, i.e. $J_{net}=IL_{net}\times J_{ph,cell}$ (1Sun), we can calculate this new magnitude considering both IL_{cell} and the solar cell dynamics as

$$IL_{net} = IL_{cell} - \frac{C_D \frac{dV'}{dt}}{J_{ph,cell}(1Sun)} \quad (3)$$

Notice that IL_{net} can be obtained just by measuring the light intensity that illuminates the cell and the evolution of the V_{oc} with time, and then $pJ_{dark}=J_{net}$ can be calculated. It is important to observe that eq. (2) and (3) assume proportionality between cell photocurrent and the irradiance level. This relation cannot be held when carrier collection depends on the voltage. This phenomenon can arise due to an effective lifetime with a strong injection level dependence.

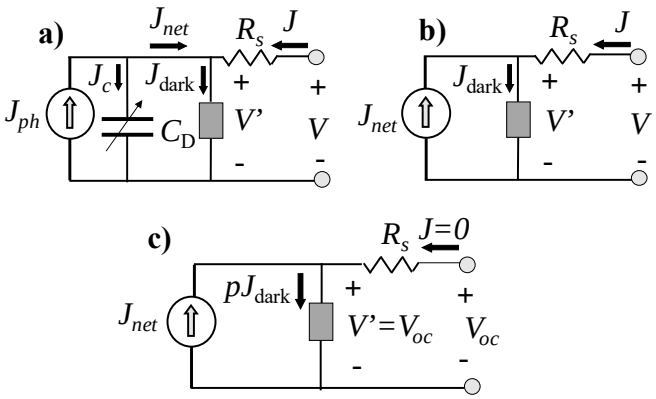

Fig. 2. a) Dynamic electrical model of a solar cell with series resistance R_s. b) Simplified model using the net current density (J_{net}) concept. c) The corresponding model in open circuit conditions.

As a main result of Suns-V_{oc} measurements, the pJ_{dark} and pJ_{light} current density vs. V_{oc} curves are achieved as are shown in Fig. 3. Finally, knowing IL_{net} a pseudo-illuminated current density can be also extracted as follows

$$pJ_{light} = J_{ph,cell}(1Sun)\times(1-IL_{net}) \tag{4}$$

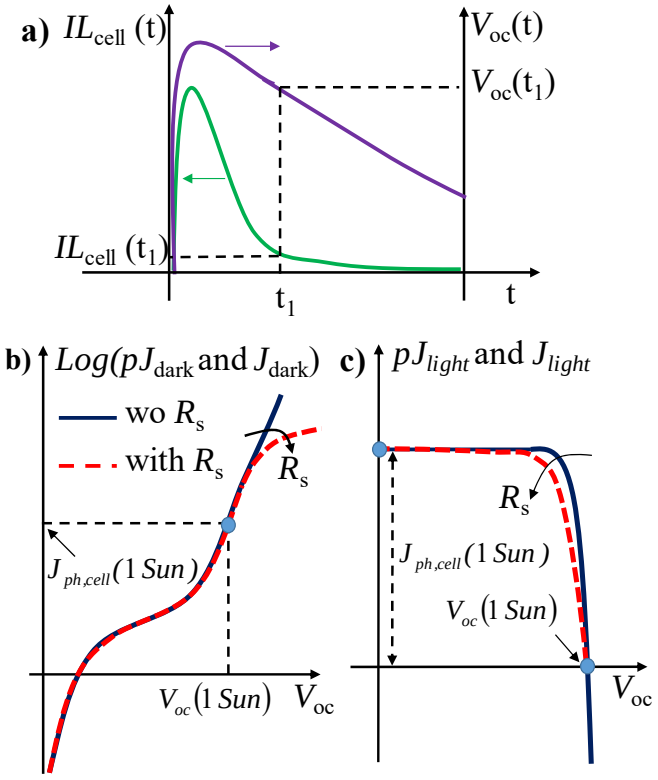

Fig. 3. a) Temporal evolution of IL_{cell} and V_{oc} after a flash shot (linear axes). b) Typical pJ_{dark} and c) pJ_{light} curves compared with the corresponding J_{dark} and J_{light} curves considering ohmic series losses, in semilog and linear axes respectively.

As a result, pJ_{dark}-V_{oc} and pJ_{light}-V_{oc} curves can be obtained as it is illustrated in fig. 3. For every instant of time V_{oc} and IL_{cell} are recorded. From these values and using equation (3), the corresponding IL_{net} is calculated which leads to pJ_{dark} and pJ_{light}. These magnitudes are then plotted vs. V_{oc} values leading to the curves shown in fig. 3b and 3c, where the effect of R_s is also indicated.

III. SYSTEM IMPLEMENTATION

The Suns-V_{oc} system consists basically of four elements as can be seen in Fig. 1, namely: 1) a flash lamp with external ignition control, 2) a digital programmable oscilloscope, 3) a photodetector circuit including photodiodes and auxiliary electronics and 4) a computer to control the whole system using a commercial windows based spreadsheet program, which configures and controls both the oscilloscope and the photodetector subsystems using Visual Basic for Applications (VBA) scripts that rely on NI-VISA drivers. Measured data results are directly uploaded, processed and plotted in the same spreadsheet environment following the acquisition flow chart diagram shown in Fig. 4. All the elements, except for the flash-lamp, use the universal serial bus (USB) interface for communication and programming purposes. In addition, the USB port also provides the power supply to the photodetector circuit.

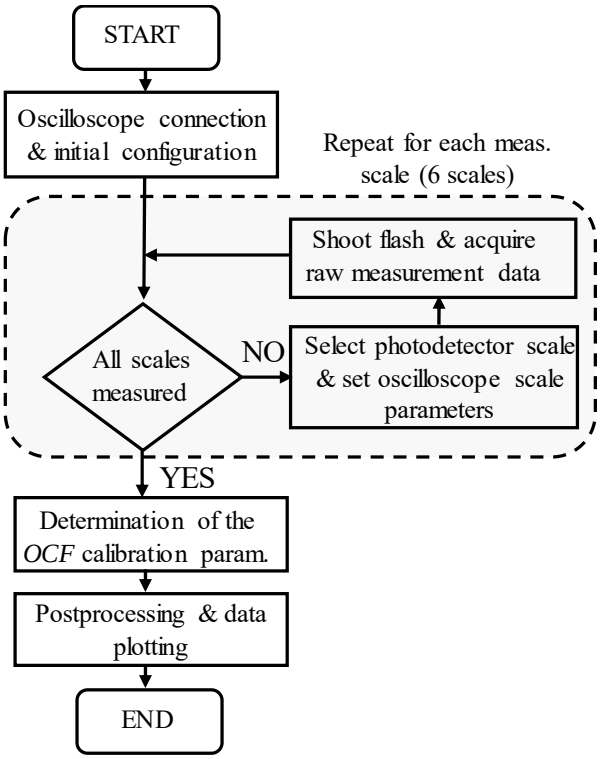

Fig. 4. Data acquisition flow chart diagram during Suns-V_{oc} measurements.

Among those components, the photodetector is the most important block in our Suns-V_{oc} system (see Fig. 5). The detector circuit incorporates three reverse biased c-Si photodiodes of different active area sizes (0.8, 5.1 and 100 mm^2) implementing a total of six irradiance level scales, from i=1 to 6, where the letter "i" is an integer number as scale label. In this way, we can sweep seven magnitude orders in light intensity from 10^2 to 10^{-5} Suns. Reverse bias voltage is adjusted to 4.8 V for the small and middle photodiodes, and 3 V for the largest photodiode using two linear regulators from the 5 V voltage supply provided by the USB port. Notice that photodiodes are based on c-Si material, then the system designed hereby is well suited for measuring c-Si solar cells in order to have a similar response under flash-lamp light spectrum. Every scale is chosen using an analogue multiplexer and switching-on a n-channel MOSFET transistor by means of a control voltage ($V_{ctrl,i}$). In this way, a single photodiode together with a specific load resistor is selected. For every scale, the resistor $R_{L,i}$ value allows to adjust the current-voltage gain, i.e. the Suns/V calibration factor.

The measured voltage in each resistance ($V_{det,i}$) is directly related to the measured light irradiance level ($IL_{det,i}$) as follows

$$IL_{det,i} = \frac{V_{det,i}}{R_{L,i} \times I_{ph,det\_i}(1\ Sun)} \quad (5)$$

where I_{ph,det_i} (1Sun) is the photodiode photocurrent measured previously at one Sun using a solar simulator (AM1.5G 1 kW/m^2 solar spectrum) as a calibration factor.

The photodetector electronics is controlled by a µ-controller unit integrated in the same circuit (µc-unit block in Fig.5a). Each scale is designed to guarantee that the selected photodiode works in the photoconductive region, i.e. reverse biased, where the photocurrent of the photodiode is proportional to the irradiance level, i.e. $I_{ph,det\_i}=IL_{det,i}\times I_{ph,det\_i}$ (1Sun). It is important to remark that $IL_{det,i}$ can be different from IL_{cell} due to a non-uniform light spot or/and different flash-lamp distance between detector and solar cell under test in the measurement setup. For this reason, an optical correction factor (*OCF*) is necessary to be included in eq. (5) in order to calculate IL_{cell} as $IL_{det,i}/OCF$. The *OCF* parameter is automatically calculated by the system once the $J_{ph,cell}$ (1Sun) and V_{oc} (1Sun) of the solar cell under test are provided.

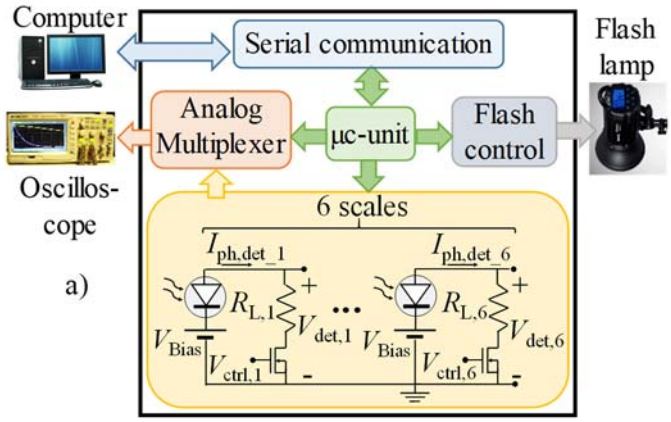

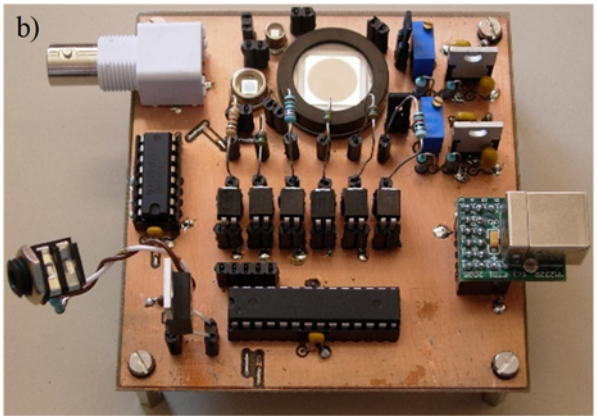

Fig. 5. a) Simplified electronic scheme of the photodetector circuit. b) The implemented photodetector circuit.

Additionally, every photodetector circuit scale is designed to respond very fast in comparison with the flash light decay. In this way, the time constant of the detector circuit (τ_{RC}) calculated as $\tau_{RC}=C_{ph,I}\times R_{L,i}$ (photodiode capacitance ($C_{ph,i}$) was measured by impedance spectroscopy in the whole reverse bias voltage range) is at least 27 times lower than the flash light decay time (τ_{flash}~1.8 ms) independently of the scale, as can be seen in table I. The flash illumination pulse has a duration of around 30 ms as can be seen in Fig. 6.

TABLE I. INSTRUMENT SCALES AND PARAMETERS RELATED TO EACH ONE, NAMELY: PHOTODIODE SIZE, LOAD RESISTANCE, V/SUNS CALIBRATION FACTOR. THE FLASH AND DETECTOR CIRCUIT TIME CONSTANT RATIOS ARE SHOWN IN THE LAST COLUMN

Scale label	Scale (Suns)	Phot. size (mm^2)	R_L (Ω)	V/Suns	τ_{Flash}/τ_{RC}
1	$>10^1$	0.8	120	0.044	$7.5\cdot10^5$
2	10^1-10^0	5.1	120	0.240	$3.0\cdot10^5$
3	10^0-10^{-1}	5.1	1200	2.40	$3.0\cdot10^4$
4	10^{-1}-10^{-2}	100	820	24.2	$7.3\cdot10^2$
5	10^{-2}-10^{-3}	100	4700	139	$1.3\cdot10^2$
6	$<10^{-3}$	100	22000	651	$2.7\cdot10^1$

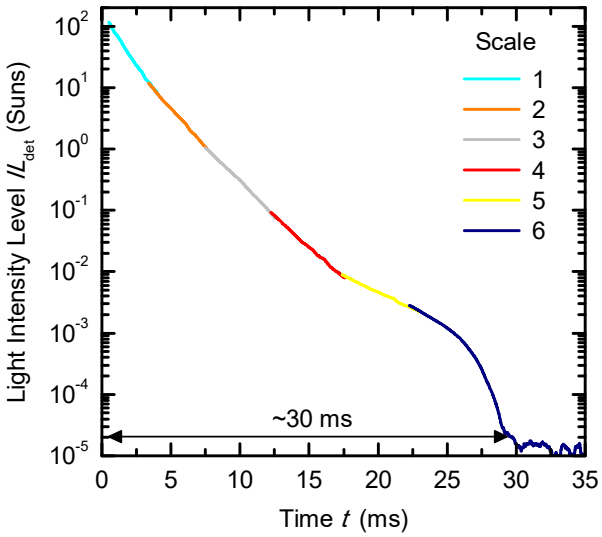

Fig. 6. (color online) Irradiance level measured by the detector after a flash light spot of about 30 ms. This curve was achieved considering the whole measurement range using the six scales of the instrument.

IV. RESULTS

To test the Suns-V_{oc} system, a 9 cm^2 interdigitated back-contacted (IBC) c-Si solar cell with a photovoltaic efficiency of 20.5% was used. The device was processed on <100> p-type crystalline silicon substrate (2.5 Ωcm resistivity and 260 µm thick) following a similar fabrication process described in [16, 17]. In Fig. 7 and Fig. 8 the measured pJ_{dark} and pJ_{light} curves are directly compared with the corresponding counterpart curves considering ohmic losses. As it can be seen, useful data are obtained for more than 6 orders of magnitude with excellent matching between both curves. Deviation at high injection levels is attributed to series resistance effect, while at low injection levels we can see a constant pJ_{dark} value related to the noise floor of the photodetector channel at the lowest scale.

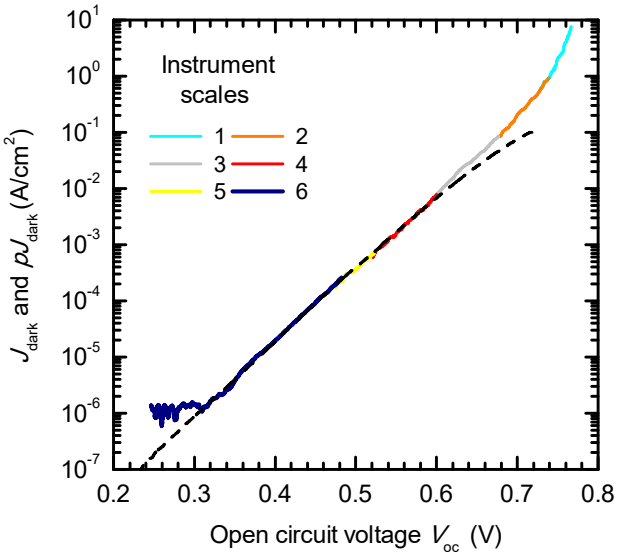

Fig. 7. (color online) pJ_{dark} (continuous color lines) and J_{dark} (black dashed line) vs. V_{oc} curves for a lab IBC solar cell.

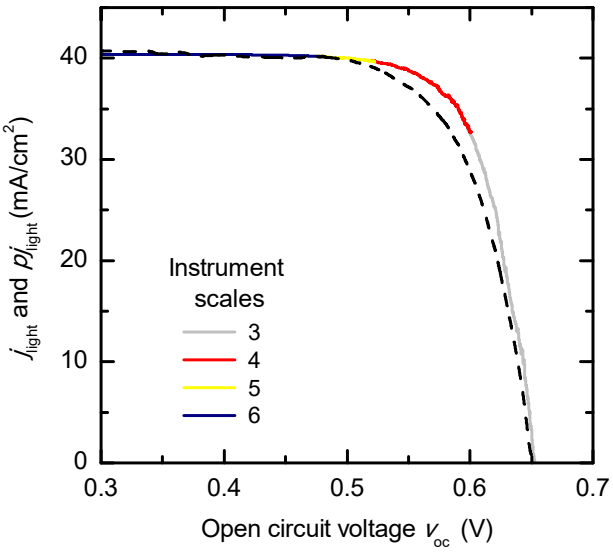

Fig. 8. (color online) pJ_{light} (continuos color lines) and J_{light} (dashed black line) vs. V_{oc} curves for the measured IBC cell working at 1 Sun (1 kW/m^2).

From the pJ_{light} curve, the so called pseudo power density curve (pP_{light}) can be achieved by multiplying pJ_{light} by V_{oc}, as is shown in Fig. 9. Notice that the shape of both pJ_{light} and pP_{light} curves in Fig. 8 and 9 respectively, is similar to the shape of the conventional J_{light}-V and P_{light}-V curves of a photovoltaic device. Nevertheless, each point of the pseudo curves corresponds to an irradiance that is different from the next point, instead of the conventional case where the irradiance is the same along the single curve.

By analyzing the pP_{light} curve, the pseudo Fill Factor (pFF) and the pseudo efficiency ($p\eta$) of the cell without the R_s effect can be extracted. Table II summarizes the photovoltaic parameters of the measured IBC solar cell.

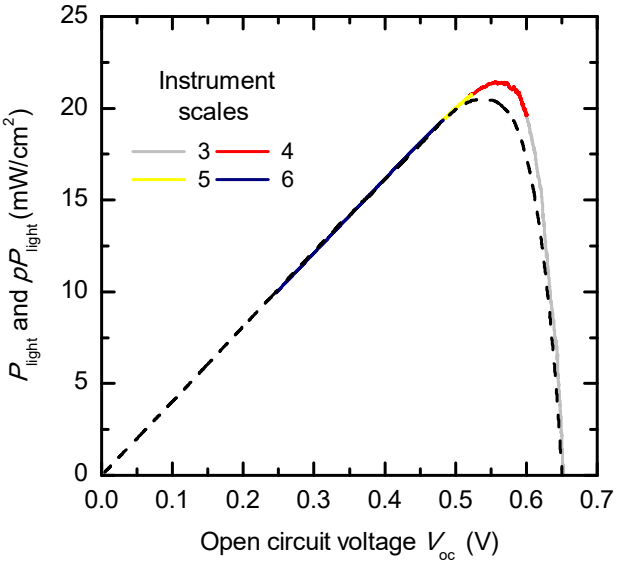

Fig. 9. (color online) pP_{light} (continous color lines) and P_{light} (dashed black line) vs. V_{oc} curves for the measured IBC cell working at 1 Sun (1 kW/m^2). P_{light} curve takes into account the effect of R_s.

TABLE II. MEASURED PHOTOVOLTAIC PARAMETERS

$J_{ph,cell}$ (1Sun) (mA/cm^2)[a]	V_{oc} (1Sun) (mV)[a]	FF (%)[a]	pFF (%)[b]	$p\eta$ (%)[b]	η (%)[a]
40.4	651	78.1	81.6	21.5	20.5

[a]Measured with a solar simulator under AM1.5G 1 kW/m^2 solar spectrum T=25ºC
[b]Extracted from Suns-V_{oc} measurements

An estimation of the series resistance of the cell working around the maximum power point at 1 Sun can be calculated using eq. (6) [18]. For example, considering data from Table II a R_s value of 0.69 Ωcm^2 is extracted for our measured IBC solar cell.

$$R_s \cong \left(1 - \frac{FF}{pFF}\right) \frac{V_{oc}\,(1\,Sun)}{J_{ph,cell}\,(1\,Sun)} \qquad (6)$$

One of the main advantages of the Suns-V_{oc} technique is the possibility to extract the effective lifetime (τ_{eff}) of the solar cell vs. excess carrier density (Δn) once the device is finished. Along the solar cell fabrication process, typically this information is measured through the well-known quasi-steady-state photoconductance method (QSS-PC) [19]. However, this technique cannot be applied once the solar cell is metallized. The τ_{eff} vs. Δn dependence can be extracted using eq. (7) and (8) [5, 6] and the obtained curve for the IBC cell is shown in Fig. 10.

$$\Delta n = \frac{-N_{Dop} + \sqrt{N_{Dop}^2 + 4n_i e^{\frac{V_{oc}}{V_T}}}}{2} \tag{7}$$

$$\tau_{eff} = \frac{\Delta n}{\frac{IL_{cell} \times J_{ph,cell}(1Sun)}{qw} - \frac{\partial \Delta n}{\partial t}} \tag{8}$$

As it can be seen, due to the extended irradiance range, reliable τ_{eff} values can be obtained up to $\Delta n = 10^{10}$ cm^{-3}. Notice that in our device, carrier lifetimes are well below the flash light decay time (~1.8 ms), so solar cell capacitive dynamics has a negligible impact on the measurements, i.e. $IL_{net} \cong IL_{cel}$.

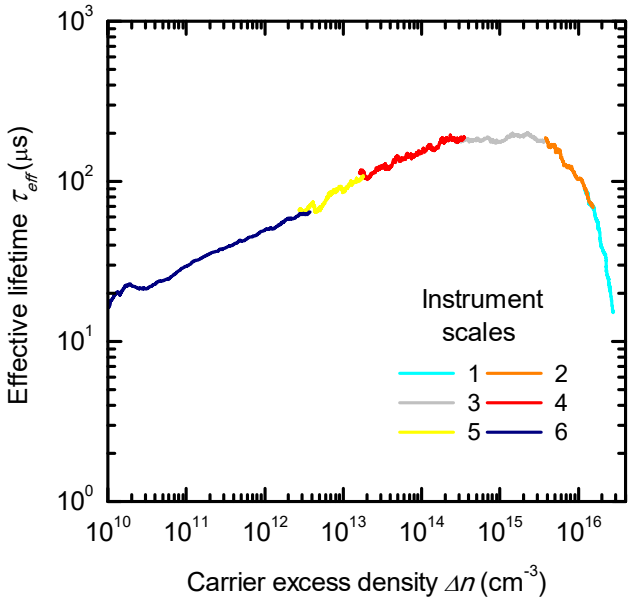

Fig. 10. (color online) τ_{eff}-Δn curve from Suns-V_{oc} measurements of the finished lab IBC solar cell.

V. Conclusion

In this work we have demonstrated the viability of a Suns-V_{oc} instrument to characterize c-Si solar cells with enough sensitivity to cover a wide irradiance range from 10^{-5} to 10^{2} Suns. From the point of view of theoretical interpretation, equations that are behind the measurement technique are reinterpreted in a novel electrical solar cell model to take into account the dynamic behavior of the device using the QSS-V_{oc} method. Pseudo dark and pseudo light current density-voltage curves as well as the pseudo fill factor and pseudo efficiency of the measured solar cells are achieved automatically in a very short time. Additionally, the effective lifetime vs. carrier excess density curve calculated from the measured data can be extended to very low injection levels. The instrument has been successfully tested in an interdigitated back contacted c-Si(p) solar cell (9 cm^2 area) allowing accuracy current densities measurements in the 10^{-6} to 10 A/cm^2 range with a pseudo fill factor and efficiency without considering ohmic losses of 81.6% and 21.5% respectively. Moreover, effective lifetimes values are reliable up to carrier excess densities of 10^{10} cm^{-3}.

AKNOWLEDGMENT

This work was supported in part by the Spanish Government under a FPU grant (FPU13/04381), and projects ENE2016-78933-C4-1-R, ENE2017-87671-C3-2-R and TEC2017-82305-R. The work was also supported in part by the project REFER COMRDI15-1-0036 funded by ACCIÓ and the European Regional Development Fund (FEDER). The authors wish to thank Mr. Miguel Garcia for its help in the mechanical and electrical photodetector interface development.

REFERENCES

[1] M.D. Yandt, J.P.D. Cook, M. Kelly, H. Schriemer, and K. Hinzer, "Dynamic real time I-V curve measurement system," *IEEE J. Photovoltaics*, vol. 5, no.1, pp. 337-343, 2015.

[2] S.R.G. Hall, M. Cahmore, J. Blackburn, G. Koutsourakis, and R. Gottschalg, "Compressive current response mapping of photovoltaic devices using MEMS mirror arrays," *IEEE Trans. Instrum. Meas*., vol. 65, no. 8, pp. 1945-1950, 2016.

[3] E. López-Fraguas, J.M. Sánchez-Pena, and R. Vergaz, "Low-cost LED solar simulator," Accepted in *IEEE Trans. Instrum. Meas*., DOI: 10.1109/TIM.2019.2899513, 2019.

[4] A. Nedungadi, and R. Shararn, "A Simple Parameter Measurement System for Solar Cells," *IEEE Trans. Instrum. Meas*., vol. IM-31, no. 3, pp. 206-207, 1982.

[5] M.J. Kerr, and A. Cuevas, "Generalized analysis of the illumination vs. open-circuit voltage of solar cells," *Solar Energy*, vol. 76, pp. 263-267, 2004.

[6] M.J. Kerr. A. Cuevas, and R.A. Sinton, "Generalized analysis of quasy-steady-state and transient decay open circuit voltage measurements," *J. Appl. Phys.*, vol. 91, no. 1, pp. 399-404, 2002.

[7] S.W. Gunz, J. Nekarda, H. Mäckel, and A. Cuevas, "Analyzing back contacts of silicon solar cells by suns-voc-measurements at high illumination densities," in *Proc. 22nd European Photovoltaic Solar Energy Conference and Exhibition*, Milan, Italy, pp. 849-853, 2007.

[8] N.S. Beattie, G. Zoppi, P. See, I. Farrer, M. Duchamp, D.J. Morrison, R.W. Miles, and D.A. Ritchie, "Analysis of InAs/GaAs quantum dot solar cells usin Suns-V_{oc} measurements," *Sol. Energy Mater. Sol. Cells*, vol. 130, pp. 241-245, 2014.

[9] S. Schiefer, B. Zimmermann, S.W. Glunz, and U. Würfel, "Applicability of the Suns-V_{oc} method on organic solar cells" *IEEE J. Photovolt.*, vol. 4, no. 1, pp. 271-277, 2014.

[10] O. Gunawan, T. Gokmen, and D.B. Mitzi, "Suns-Voc characteristics of high performance kesterite solar cells," *J. Appl. Phys.*, vol. 116, Art. no. 084504, 2014.

[11] H. Hidayat, P.I. Widenborg, and A.G. Aberle, "Large-area Suns-V_{oc} tester for thin-film solar cells on glass superstrates," *Energy Procedia*, vol. 15, pp. 258-264, 2012.

[12] R. A. Sinton, and A. Cuevas, "Contactless determination of current–voltage characteristics and minority-carrier lifetimes in semiconductors from quasi-steady-state photoconductance data," *Appl. Phys. Lett.*, vol. 69, no. 17, pp. 2510, 1996

[13] J. Schmidt, and A.G. Aberle, "Accurate method for the determination of bulk minority-carrier lifetimes of mono- and multicrystalline silicon wafers," *J. Appl. Phys.*, vol. 81, no. 9, pp. 6186, 1997.

[14] I. Mora-Seró, G. Garcia-Belmonte, P.P. Boix, M. A. Vázquez, and J. Bisquert, "Impedance spectroscopy characterisation of highly efficient silicon solar cells under different light illumination intensities," *Energy Environ. Sci.*, vol. 2, pp. 678-686, 2009.

[15] Sinton Instruments. *Suns-Voc-Post-Diffusion Process Control*. Accesed: March, 10, 2019. [Online]. Avalaible: www.sintoninstruments.com/products/suns-voc/

[16] E. Calle, P. Ortega, G. López, I. Martín, D. Carrió, G. Masmitjà, C. Voz, A. Orpella, J. Puigdollers, and R. Alcubilla, "Interdigitated back-contacted c-Si(p) solar cells with photovoltaic efficiencies beyond 22%," in *Proc. 11th Spanish Conference on Electron devices (CDE 2017)*, Barcelona, Spain, 2017. [Online] Avalaible: https://doi.org/10.1109/CDE.2017.7905230, 2017.

[17] P. Ortega, E. Calle, G. von Gastrow, P. Reppo, D. Carrió, H. Savin, and R. Alcubilla, "High-efficiency black silicon interdigitated back contacted solar cells on p-type and n-type c-Si substrates," *Prog. Photovolt.: Res. Appl.*, vol. 23, pp. 1448-1457, 2015.

[18] M. Green, "Solar cells: operating principles, technology and systems applications," *Englewood Cliffs*, NJ, USA: Prentice-Hall Inc., 1982, pp. 97.

[19] A. Cuevas, and D. Macdonald, "Measuring and interpreting the lifetime of silicon wafers," *Solar Energy,* vol. 76, pp. 255-262, 2004.